CRYSTAL GROWTH & DESIGN

Article

Crystal Engineering of 1-Halopolyynes by End-Group Manipulation

Bart#omiej Pigulski, Nurbey Gulia, Patrycja M#cik, Robert Wieczorek, Agata Arendt, and Slawomir Szafert

Cryst. Growth Des., **Just Accepted Manuscript** • DOI: 10.1021/acs.cgd.9b00987 • Publication Date (Web): 18 Sep 2019

is published by the American Chemical Society. 1155 Sixteenth Street N.W., Washington, DC 20036

Crystal Engineering of 1-Halopolyynes by End-Group Manipulation

AUTHOR NAMES Bartłomiej Pigulski, Nurbey Gulia, Patrycja Męcik, Robert Wieczorek, Agata Arendt, Sławomir Szafert**

AUTHOR ADDRESS Faculty of Chemistry, University of Wrocław, 14 F. Joliot-Curie, 50-383 Wrocław, Poland

KEYWORDS polyynes, halogen bond, alkynes, X-ray crystallography

ABSTRACT

Polyynes are compounds with two or more conjugated carbon-carbon triple bonds. Such molecules are usually regarded as models of carbyne – hypothetical one-dimensional allotropic form of carbon. 1-Halopolyynes are rare representatives of such species but few interesting crystal-to-crystal reactions have been lately reported for them. Herein, we present 11 new X-ray structures of 1-halopolyynes nearly doubling the number of such compounds characterized with the use of single crystal X-ray diffraction. The influence of an end-group on packing motifs in crystal structures of the 1-halopolyynes were thoroughly examined. Especially the strength of halogen bond as a function of polyyne chain length was analyzed with the support of theoretical calculations. Moreover, compound **CNC_8I** is the longest 1-halopolyyne characterized to date with the use of rentgenostructural analysis. In addition to that, compounds **NO_2C_6Br** and **$MeC(O)C_6Br$** are the first 1-bromohexatriynes characterized by means of X-ray single crystal diffraction.

INTRODUCTION

The synthesis and properties of polyynic compounds – exciting linear carbon rods – have been attracting an interest of scientific community for a long time.[1-4] Polyynes are usually regarded as mimics of hypothetical linear allotropic form of carbon – carbyne. This makes the exploration of spectroscopic and structural properties of such carbon rods a very attractive task. Crystallographic studies of longer polyynes gives very valuable insight into possible structure of carbyne.[5-6] For instance, Tykwinski and co-workers reported a significant reduction in the bond length alternation as a function of the polyyne length and such trend seems to be saturated before cumulenic structure is achieved.[7] Moreover, polyynes might be used as valuable precursors in various chemical transformation.[8] They also possess a significant potential as molecular wires and switches,[9-13] NLO (nonlinear optics) materials,[14-20] or even in live-cells imaging and sorting.[21] It is worth to note that such unusual structural motif may be found in many natural products.[22] Theoretical calculations reported by Yakobson and co-workers suggest that carbyne might be about twice as stiff as the stiffest known materials.[23] Isolation of exceptionally long carbon chains encapsulated in double-walled carbon nanotubes (polyynes@DWCNTs) was recently reported and it gives hope that bulk carbyne might be accessible someday.[24] Moreover, the formation of polyynes induced by atomic manipulation of their dibromoolefin precursors has been reported very recently.[25]

Our recent research has been focused on 1-halopolyynes i.e. polyynes that contain at least one halogen end-group. Such compounds exhibit unusual reactivity in for instance mechanoactivated coupling with pyrroles,[26-27] allow for the formation of amine end-capped polyynes[28-31] or might be used in the synthesis of fluorescent dyes.[32] Moreover, 1-halopolyynes are versatile substrates for palladium(II)[33-34] or iridium(III) end-capped polyynes.[35] Examples of X-ray structures of 1-halopolyynes, especially homologs longer than butadiyne, are rather sparse. According to the CSD,[36] for now only one structure containing

$(C\equiv C)_2Cl$ structural motif[37] and four structures containing $(C\equiv C)_2Br$[38-40] motif are known. Moreover, 11 structures with $(C\equiv C)_2I$ motif[37,41-46] and 3 with $(C\equiv C)_3I$[42,47] motif were reported. Except for one 1-iodobutadiyne structure[37] all the others are different cocrystals of $I(C\equiv C)_nI$ (n = 2, 3). Structures of pure $I(C\equiv C)_nI$ compounds are not known due to the fact that they form needle-like crystals that are disordered along one axis.[43] Despite the rarity of 1-halopolyynes, some interesting crystal-to-crystal transformations of such compounds have been reported. For instance, Frauenrath and co-workers discovered unprecedented crystal-to-crystal dimerization of 1-bromobutadiyne that involves unusually large atom displacements associated with bond cleavage and formation of new bonds (Scheme 1, upper left part).[38] It is noteworthy, that it was possible to measure X-ray single crystal structure before and after the reaction. Similar reaction was carried out for 1-bromohexatriyne but only microcrystalline samples were obtained (Scheme 1, upper right part).

Halogen bond is an extremely powerful tool that may be used in crystal engineering.[48] Goroff and co-workers reported topochemical polymerization of diiododiacetylene templated by Lewis base host molecules (Scheme 1, down).[43,49] Strong halogen bond between diiodobutadiyne and the host molecules forced butadiyne molecules to adopt geometry appropriate for such polymerization. As a result, poly(diiododiacetylene) (PIDA) was obtained. The same strategy was next used for more unstable dibromodiacetylene.[39]

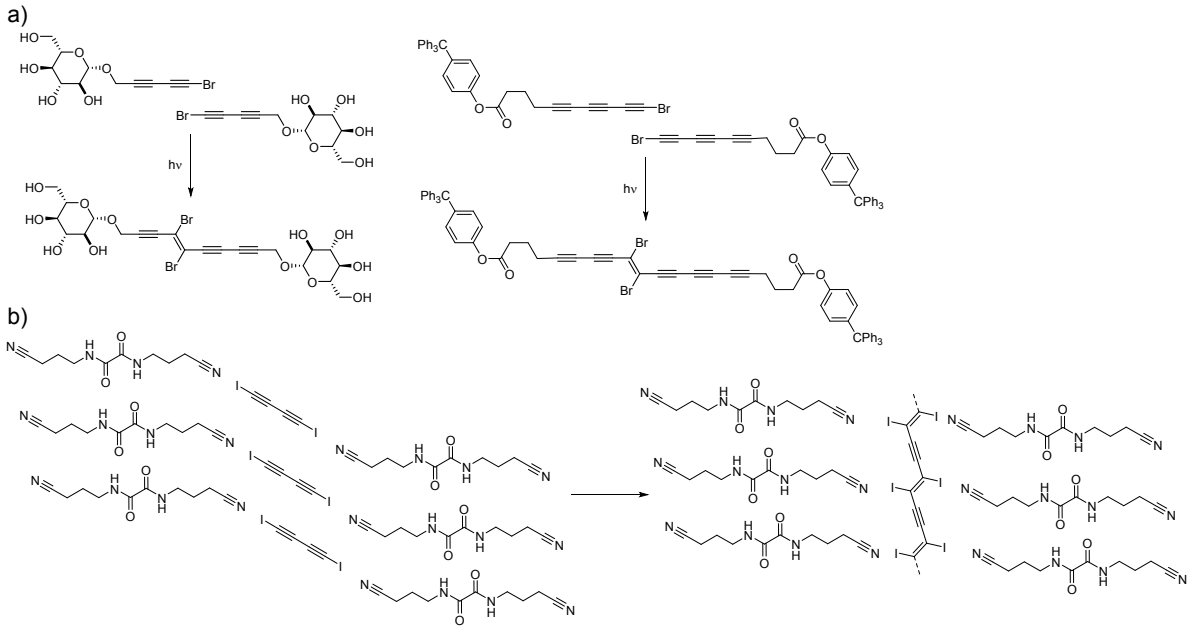

Scheme 1. Crystal-to-crystal reactions of 1-halopolyynes: a) dimerization of 1-bromobutadiyne and 1-bromohexatriyne; b) polymerization of diiododiacetylene templated by Lewis base host molecule.

The abovementioned examples of an extraordinary crystal-to-crystal reactivity of 1-halopolyynes makes an understanding of factors that allow to control packing motifs of such molecules what is very valuable in a context of crystal engineering.

Herein we report 11 new structures of 1-halopolyynes nearly doubling the number of such compounds characterized with the use of single crystal X-ray diffraction. The use of one non-halogen end-group allowed to obtain crystal structures of pure 1-halopolyynes to be compared with the $X(C{\equiv}C)_nX$ series. Moreover, structure of **CNC_8I** is the only known structure of 1-halooctatetrayne. In addition to that, thorough analysis of packing motifs and intermolecular interactions was performed. Especially an influence of linear carbon chain on C-X bond as well as on intermolecular halogen bonds was investigated.

EXPERIMENTAL SECTION

General. All reactions were conducted under N_2 with the use of standard Schlenk techniques. Glassware was pre-dried at 120 °C. Solvents were treated as follows: hexane was distilled from Na, THF was distilled from Na/benzophenone, CH_2Cl_2 was distilled from P_2O_5, and CH_3CN (HPLC grade) was used as received. Known 1-halopolyynes[27,33-34,50] and 1-haloalkynes (1-(bromoethynyl)-4-fluorobenzene and 1,2,3,4,5-pentafluoro-6-(iodoethynyl)benzene[51-52] were obtained according to the known procedures. CuI (Aldrich, 99%), $Pd(PPh_3)_2Cl_2$ (Aldrich, 98%), diisopropylamine (Aldrich, 99.5%), AgF (Alfa Aesar, 98%), NIS (*N*-iodosuccinimide, Alfa Aesar, 97%), trimethylsilylacetylene (Fluorochem, 98%) were used as received.

^1H, ^{13}C and ^{19}F NMR spectra were recorded on a Bruker Avance 500 spectrometer. For all the ^1H NMR spectra, the chemical shifts are given in ppm relative to the solvent residual peaks. For ^{13}C NMR spectra, the chemical shifts are given in ppm relative to the solvent peaks ($CDCl_3$, ^1H: 7.26 ppm, ^{13}C: 77.2 ppm,). For the ^{19}F NMR spectra, hexafluorobenzene was used as an internal standard (-165 ppm). Coupling constants are given in Hz. HRMS spectra were recorded using Bruker apex ultra FT-ICR and MicOTOF-Q spectrometers with ESI ion source. IR spectra were recorded using a Bruker 66/s FTIR spectrometer. Microanalyses were conducted with an Elementar CHNS Vario EL III analyzer.

X-ray single crystal diffraction.

The structurally analyzed compounds were crystallized from their hexane or hexane/CH_2Cl_2 solutions. X-ray diffraction data were collected with a Kuma KM4 CCD of Xcalibur Onyx (ω scan technique) diffractometers. The space groups were determined from systematic absences and subsequent least-squares refinement. Lorentz and polarization corrections were applied. The structures were solved by direct methods and refined by full-matrix, least-squares on F^2 by use of SHELXTL package.[53] Non-hydrogen atoms were refined with anisotropic thermal

parameters. Hydrogen atom positions were calculated and added to the structure factor calculations, but were not refined. Absorption corrections were applied with the use of CrysAlisPRO.[54] Mercury 3 software was used for crystal and molecular structures plots.[55]

Computational details.

The molecular orbital studies on isolated molecules of **MeC(O)C_4Cl**, **MeC(O)C_4Br**, **MeC(O)C_6Br**, **CNC_4I**, **CNC_6I**, **CNC_8I**, **NO_2C_4I**, **NO_2C_4Br**, **NO_2C_6Br**, **$C_6F_5C_6$I** and **FC_4I** compounds have been performed at the DFT level of theory. Gaussian 09 C.01[56] suite of programs using the ωB97X-D[57] long-range corrected hybrid density functional with damped atom-atom dispersion corrections was used with DGDZVP for Cl, Br, I and 6-311G(2d,2p) for N, O, C, H atoms basis set. All presented structures are fully optimized with tight (as defined in Gaussian) convergence criteria. All isolated molecules are thermodynamically stable. The atomic charges have been calculated on the base of full NBO analysis, the CHELPG (Charges from Electrostatic Potentials using a Grid based method) with scheme by Merz, Singh and Kollman[58-59] with fitting atom radii using Universal Force Field.[60] The molecular electrostatic potential (MEP) as a predictive reactivity factor of the molecule has been presented on isosurface of the total electron density 0.0004 e/au^3 using the GaussView 5.08 software.[61]

Hirshfeld Surface Analysis. Hirshfeld surfaces and the fingerprint plots were generated using CrystalExplorer,[62] which utilizes a structure input file in CIF format. The distance from the Hirshfeld surface to the nearest atoms outside and inside the surface are characterized by the d_e (external) and d_i (internal) values, respectively. The normalized contact distance based on these values is d_{norm}= $(d_i - r_i\text{vdW})/r_i\text{vdW} + (d_e - r_e\text{vdW})/\text{r}_\text{e}\text{vdW}$, where $r_i$vdW and $r_e$vdW are the van der Waals radii of the external and internal atoms. The d_{norm} is encoded on

Hirshfeld surface with colors: red – the highest value, blue – the lowest value. The 2D histograms, with fingerprints, plot d_e versus d_i.

Syntheses.

((4-Fluorophenyl)buta-1,3-diyn-1-yl)trimethylsilane (FC_4TMS)

1-(Bromoethynyl)-4-fluorobenzene (0.769 g, 3.86 mmol) was dissolved in 40 mL of dry and oxygen-free THF and then ethynyltrimethylsilane (0.82 mL, 5.7 mmol), CuI (0.029 g, 0.15 mmol), and $Pd(PPh_3)_2Cl_2$ (0.055 g, 0.31 mmol) were added. Next diisopropylamine (1.37 mL, 9.66 mmol) was added dropwise and then the mixture was stirred for 3.5 h under N_2. The solvent was removed under reduced pressure and the residue was purified by silica gel chromatography (hexanes) yielding 0.279 g (1.29 mmol) of white solid. Yield 33%. ^{1}H NMR (500 MHz, $CDCl_3$): δ = 7.49 – 7.45 (m, 2H , H_{Ar}), 7.04 – 6.98 (m, 2H, H_{Ar}), 0.23 (s, 9H, $Si(CH_3)_3$); ^{13}C NMR (126 MHz, $CDCl_3$): δ = 163.3 (d, J_{CF} = 251.8 Hz), 134.9 (d, J_{CF} = 8.6 Hz), 117.6 (d, J_{CF} = 3.6 Hz), 116.0 (d, J_{CF} = 22.2 Hz), 90.9 (s), 87.8 (s), 75.8 (s), 74.1 (d, , J_{CF} = 1.6 Hz), -0.3 (s); ^{19}F NMR (471 MHz, $CDCl_3$): δ = -111.5 (m, C-F); FTIR (cm^{-1}, KBr pellet): 2208(C≡C), 2102(C≡C); Elemental analysis: Calcd for $C_{13}H_{13}FSi$: C 72.18%, H 6.06%, found: C 72.13%, H 6.34%.

Trimethyl((perfluorophenyl)hexa-1,3,5-triyn-1-yl)silane ($C_6F_5C_6TMS$)

1,2,3,4,5-Pentafluoro-6-(iodoethynyl)benzene (0.873 g, 2.751 mmol) was dissolved in 10 mL of dry and oxygen-free THF and then buta-1,3-diyn-1-yltrimethylsilane (0.403 g, 3.301 mmol), CuI (0.021 g, 0.110 mmol), and $Pd(PPh_3)_2Cl_2$ (0.039 g, 0.055 mmol) were added. Next diisopropylamine (0.97 mL, 6.86 mmol) was added dropwise and then the mixture was stirred for 1.5 h under N_2. The solvent was removed under reduced pressure and the residue was purified by silica gel chromatography (hexanes) yielding 0.199 g (0.637 mmol) of white solid. Yield 23%. ^{1}H NMR (500 MHz, $CDCl_3$): δ = 0.24 (s, $SiMe_3$, 9H); ^{19}F NMR (471 MHz, $CDCl_3$): δ = -137.2 – -137.3 (m, 2F), -152.4 (tt, J = 20.7, 2.6 Hz, 1F), -163.8 – -163.9 (m, 2F); ^{13}C NMR (126 MHz, $CDCl_3$): δ = 150.4 – 147.9 (m), 144.1 – 141.4 (m), 139.1 – 136.6 (m), 99.0 – 98.6 (m), 92.1 (s), 87.4 (s), 85.60 (q, J = 3.5 Hz), 70.4 (s), 60.1 (q, J = 3.9 Hz), 60.1

(s), -0.5 (s); IR (cm^{-1}, nujol mull): 2047 (C≡C), 2077 (C≡C); Elemental analysis: Calcd for $C_{15}H_9F_5Si$: C 57.69%, H 2.90%, found: C 57.77%, H 2.52%.

1-Fluoro-4-(iodobuta-1,3-diyn-1-yl)benzene (FC_4I)

((4-Fluorophenyl)buta-1,3-diyn-1-yl)trimethylsilane (0.079 g, 0.370 mmol) was dissolved in 10 mL of acetonitrile and next H_2O (13 μL) and AgF (0.046 g, 0.370 mmol) and NIS (0.102 g, 0.438 mmol) were added. The flask was wrapped in aluminum foil and the mixture was stirred for 2 h at room temperature. The solvent was removed under reduced pressure and the residue was purified by passing the mixture through the silica gel (hexanes:CH_2Cl_2; v/v; 1/1) yielding 0.096 g (0.35 mmol) of white solid. Yield 97%. ^{1}H NMR (500 MHz, $CDCl_3$): δ = 7.50 – 7.45 (m, 2H , H_{Ar}), 7.04 – 6.99 (m, 2H, H_{Ar}); ^{13}C NMR (126 MHz, $CDCl_3$): δ = 163.4 (d, J_{CF} = 252.0 Hz), 135.3 (d, J_{CF} = 8.6 Hz), 117.1 (d, J_{CF} = 3.6 Hz), 116.7 (d, J_{CF} = 22.3 Hz), 78.3 (s), 74.9 (d, J_{CF} = 1.6 Hz), 72.9 (s), 2.7 (s); ^{19}F NMR (471 MHz, $CDCl_3$): δ = -111.2 (m, C-F); FTIR (cm^{-1}, KBr pellet): 2208(C≡C), 2112(C≡C); Elemental analysis: Calcd for $C_{10}H_4FI$: C 44.48%, H 1.49%, found: C 44.72%, H 1.50%.

1,2,3,4,5-Pentafluoro-6-(iodohexa-1,3,5-triyn-1-yl)benzene ($C_6F_5C_6I$)

Trimethyl((perfluorophenyl)hexa-1,3,5-triyn-1-yl)silane **($C_6F_5C_6TMS$**, 0.061 g, 0.196 mmol) was dissolved in 7 mL of acetonitrile and next H_2O (7 μL), AgF (0.025 g, 0.196 mmol) and NIS (0.055 g, 0.235 mmol) were added. The flask was wrapped in aluminum foil and the mixture was stirred for 1 h at room temperature. The solvent was removed under reduced pressure and the residue was purified by elution through silica gel (hexanes) yielding 0.042 g (0.115 mmol) of yellow solid. Yield 58%. ^{19}F NMR (471 MHz, $CDCl_3$): δ = -137.11 – -137.23 (m, 2F), -152.12 (tt, J = 20.6, 2.7 Hz, 1F), -163.68 – -163.81 (m, 2F); ^{13}C NMR (126 MHz, $CDCl_3$): δ = 150.5 – 148.0 (m), 144.1 – 141.6 (m), 139.2 – 136.6 (m), 98.8 – 98.4 (m), 85.1 (q, J = 3.6 Hz), 78.7 (s), 71.1 (s), 59.4 (q, J = 3.8 Hz), 57.3 (s), 5.6 (s); IR (cm^{-1}, nujol mull): 2080 (C≡C), 2166 (C≡C); HRMS(ESI): m/z calcd for $C_{12}HF_5I$: 366.9043 [$M+H^+$]; found: 366.9037.

RESULTS AND DISCUSSION

First, we have decided to obtain a series of 1-halopolyynes with one non-halogen end group in order to be able to crystallize them without a necessity of using host molecules. That was not possible for previously reported symmetrical $X(C{\equiv}C)_nX$ molecules. Moreover, unsymmetrical 1-halopolyynes are far more stable than dihalopolyynes[34] so the synthesis and crystallization of longer 1-halopolyynes were possible. The new 1-halopolyynes **FC_4I** and **$C_6F_5C_6I$** were obtained according to standard Cadiot-Chodkiewicz/halogenation procedure. Other polyynes were known and we have reported their syntheses in recent years.[27,33-34,50] In order to investigate an impact of an end-group on a crystal structure of 1-halogenopolyynes, 11 compounds with different substituents on aryl end-group were obtained in crystalline form (Figure 1). Most of the analyzed compounds possess one end-group that is halogen bond acceptor and C≡CX end-group that is strong halogen bond donor. Thus they may be regarded as linear carbon rod-linked XB donor-acceptor molecules. Only compounds **FC_4I** and **$C_6F_5C_6I$** possess fluorinated phenyl end-groups that are not able to act as halogen bond acceptors. Another target was to determine whether the length of the polyyne chain may have an impact on the strength of halogen bond and on the packing motifs in general. The **CNC_nI** series is the most valuable here especially due to the fact that crystal structure of *para*-$NCC_6H_4C{\equiv}CI$ (**CNC_2I**) was already reported and could be included in such analysis.[51]

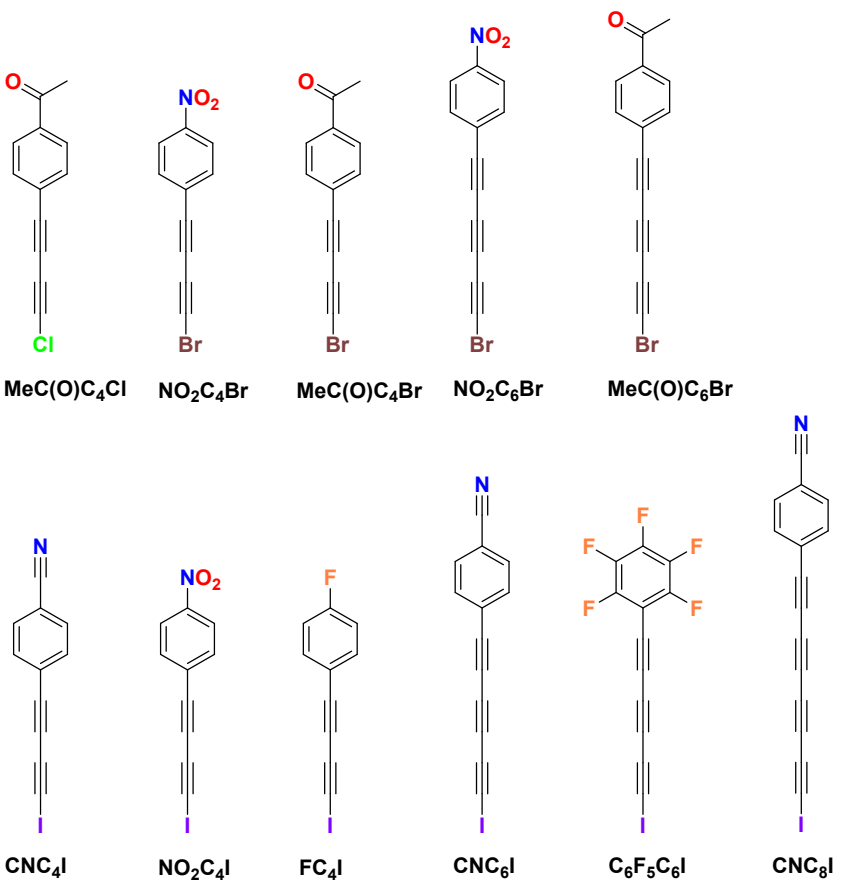

Figure 1. 1-Halopolyynes used in this study.

Molecular structure plots of all analyzed 1-halopolyynes are presented in the Supporting Information (Figures S1-S12). Summarized bond lengths in the polyyne chain are presented in the Table 1 and the contraction coefficients are presented in the Table 2. Due to resonance effect, triple bonds in such carbon rods are longer than typical "isolated" triple bond whereas single bonds are significantly shorter. This effect is observed due to some contribution of cumulene resonance form in the structure of polyynes.[5-6] Generally, longer carbon chain means longer triple bonds and shorter single bonds and it seems that this trend is saturated since certain point.[7] Moreover, longer polyynes are quite flexible systems and sp-carbon chain is very often substantially distorted.[5-6]

Contraction coefficient is a useful parameter that is used for measuring a distortion of polyyne chains (Table 2).[5-6] Such parameter may be calculated with (chain from X to C_{Ar}) or without (chain form C1-C_{Ar-1}) first atoms of end-groups (where C_{Ar-1} is the closest sp carbon

to phenyl ring, and C_{Ar} the first carbon of phenyl ring). Generally, longer polyyne chain usually means higher deformation. In the presented structures, most polyynes are almost linear (contraction coefficients in the 0.02-0.05 or 0.02-0.09% range). However, the compound **FC_4I** is rather highly distorted (contraction coefficients: 0.11% and 0.25%, respectively) despite its short butadiyne chain. Also hexatriynes **$C_6F_5C_6I$** (contraction coefficients: 0.09% and 0.16%, respectively) and **NO_2C_6Br** (contraction coefficients: 0.08% and 0.12%, respectively) are quite distorted. It is not surprising that the longest polyyne **CNC_8I** is the most distorted one with contraction coefficients 0.55% and 0.60%.

The **CNC_nI** series may be also used to investigate the influence of carbon chain length on the C-X distance (Table 1). Longer sp-carbon chain starts to be more and more electron deficient what may impact the C-I bond. Hence, known compound **CNC_2I**[51] compared with longer homologues has visibly longer C-I bond length (2.009(2) Å) and this trend seems to be present along the whole series (2.002(3) Å for **CNC_4I**, 1.991(2) Å for **CNC_6I**, 1.989(5) Å for **CNC_8I**). However, for longer compounds the differences are similar to standard deviations so we decided to perform theoretical calculations to confirm that trend. Selected calculated bond lengths for all 1-halopolyynes are in the Supporting Information (Tables S4-S7). Calculated C-I bond lengths for **CNC_nI** series are 1.999 Å for **CNC_2I**, 1.994 Å for **CNC_4I**, 1.992 Å for **CNC_6I** and 1.992 Å for **CNC_8I**. Thus theoretical calculations suggests that this trend is already saturated for **CNC_8I**. Such changes in C1-X bond length are consistent with C1 carbon chemical shift in ^{13}C NMR. Shorter C-I bond should cause stronger shielding and lower chemical shift. Indeed, ^{13}C NMR chemical shifts for *C*-I are: 13.1 ppm for **CNC_2I**,[51] 6.4 ppm for **CNC_4I**,[33] 4.2 ppm for **CNC_6I**[34] and 3.7 ppm for **CNC_8I**.[34] Opposite trend could be observed for C1-C2 bond. Shortening of C1-I bond for longer polyyne chain is associated with an elongation of C1-C2 bond. That all may be an effect of increasing contribution of cumulene resonance form in the structure of polyyne (Scheme 2). The fact of growing contribution of cumulenic resonance form along with carbon chain elongation is known and well documented.[5-7]

Table 1. Bond lengths in polyyne chains.

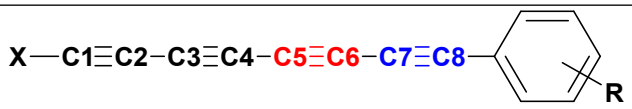

C5-C6 - only for hexatriynes and octatetrayne
C7-C8 - only for octatetrayne

Compound	Bond length [Å]								
	C1-X	C1—C2	C2—C3	C3—C4	C4—C5	C5—C6	C6—C7	C7—C8	C_{Ar-1}—C_{Ar}
$MeC(O)C_4Cl$	1.649(3)	1.194(5)	1.375(4)	1.205(5)					1.431 (4)
NO_2C_4Br	1.794(1)	1.198(2)	1.371(2)	1.209(2)					1.425 (2)
$MeC(O)C_4Br$	1.792(3)	1.198(4)	1.377(4)	1.201(4)					1.428 (4)
NO_2C_6Br	1.782(3)	1.186(4)	1.382 (4)	1.200 (4)	1.370 (4)	1.200 (4)			1.429 (4)
$MeC(O)C_6Br$ A[a]	1.796(3)	1.199(4)	1.372 (4)	1.212 (4)	1.376 (4)	1.207 (4)			1.424 (4)
$MeC(O)C_6Br$ B[a]	1.787(3)	1.202(4)	1.368 (4)	1.209 (4)	1.379 (4)	1.200 (4)			1.429 (4)
CNC_2I[25a]	2.009(2)	1.193(3)							1.438(3)
CNC_4I	2.002(3)	1.203(4)	1.377(4)	1.205(4)					1.426 (4)
NO_2C_4I	2.022(3)	1.162(4)	1.398(4)	1.200(4)					1.425 (4)
FC_4I	1.996(4)	1.211(6)	1.362(6)	1.202(6)					1.437(5)
CNC_6I	1.991(2)	1.210(2)	1.364 (2)	1.217 (2)	1.369 (2)	1.200 (2)			1.431 (2)
$C_6F_5C_6I$	1.985(3)	1.199(4)	1.374 (4)	1.207 (4)	1.365 (4)	1.207 (4)			1.424 (4)
CNC_8I	1.989(5)	1.209(6)	1.367 (7)	1.214 (7)	1.394 (7)	1.174 (7)	1.362 (7)	1.213 (7)	1.426 (6)

[a]Two molecules in the asymmetric unit.

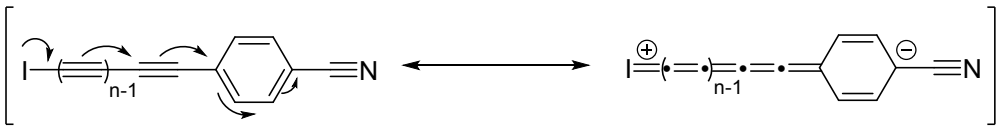

Scheme 2. Polyynic and one of the possible cumulenic resonance forms for **CNC_nI** series.

Table 2. Contraction coefficients.

	C1-C_{Ar-1}[a] [%]	X-C_{Ar}[b] [%]
CNC_4I	0	0
FC_4I	0.11	0.25
$MeC(O)C_4Br$	0.05	0.09
$MeC(O)C_4Cl$	0.05	0.07
NO_2C_4Br	0.02	0.03
NO_2C_4I	0.05	0.04

$C_6F_5C_6I$	0.09	0.16
CNC_6I	0.03	0.02
$MeC(O)C_6Br$ A[c]	0.03	0.05
$MeC(O)C_6Br$ B[c]	0.02	0.02
NO_2C_6Br	0.08	0.12
CNC_8I	0.55	0.60

[a]Contraction C1-C_{Ar-1} = ((C1-C_{Ar-1}-sum of bond lengths−C1-C_{Ar-1} distance)/C1-C_{Ar-1} sum of bond lengths)×100 %; [b]Contraction X-C_{Ar} = ((X-C_{Ar} sum of bond lengths−X-C_{Ar} distance)/X-C_{Ar} sum of bond lengths)×100 %; [c]Two molecules in the asymmetric unit.

Packing Analysis.

If substituent on an aryl group may form halogen bond with C≡CX moiety then packing motif of the crystal structure is quite predictable. The use of MeC(O)-, O_2N- or N≡C- group usually results in rather similar arrangements. In the crystal structures for **$MeC(O)C_4Cl$**, **NO_2C_4Br**, **$MeC(O)C_4Br$**, **$MeC(O)C_6Br$**, **CNC_4I**, **NO_2C_4I**, **CNC_6I** and **CNC_8I** intermolecular C≡CX···A halogen bond is the strongest intermolecular interaction (Figure 2). Linear 1-halopolyyne molecules form one-dimensional chains due to those interactions. Then, such chains are grouped into layers because of C-H···π(polyyne) interactions (Figure 2). Those layers interact with each other by stacking π···π interactions to give formally 3D-structures. A little different situation is for **NO_2C_6Br**. Here, also strong CBr···O interactions might be observed (Figure 3) but 1-halopolyyne molecules form zig-zag chains that are also grouped into layers due to C-H···π(polyyne) interactions.

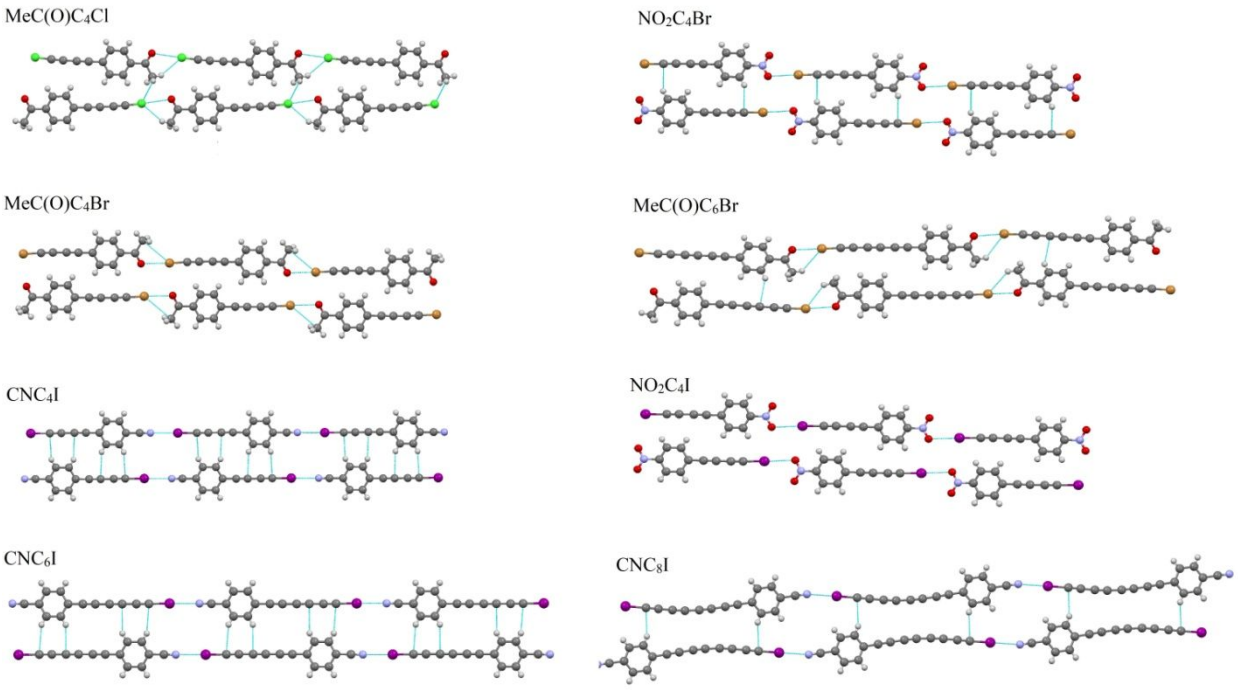

Figure 2. Crystal structures of **MeC(O)C$_4$Cl**, **NO$_2$C$_4$Br**, **MeC(O)C$_4$Br**, **MeC(O)C$_6$Br**, **CNC$_4$I**, **NO$_2$C$_4$I**, **CNC$_6$I** and **CNC$_8$I**.

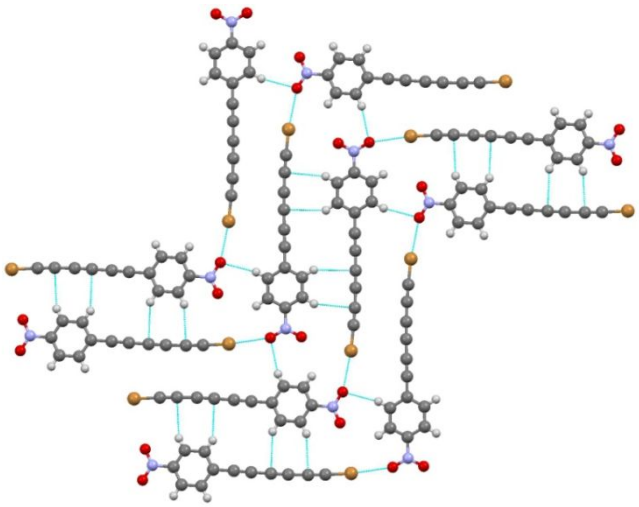

Figure 3. Crystal structure of **NO$_2$C$_6$Br**.

If there is no end-group that is halogen bond acceptor then other interactions start to play a crucial role. For instance, in the crystal structure of **FC$_4$I**, I···I interactions (3.741 Å) are present (Figure 4). Such interactions are slightly shorter than sum of van der Waals radii (3.98 Å) and facilitate formation of I···I bonded belts.

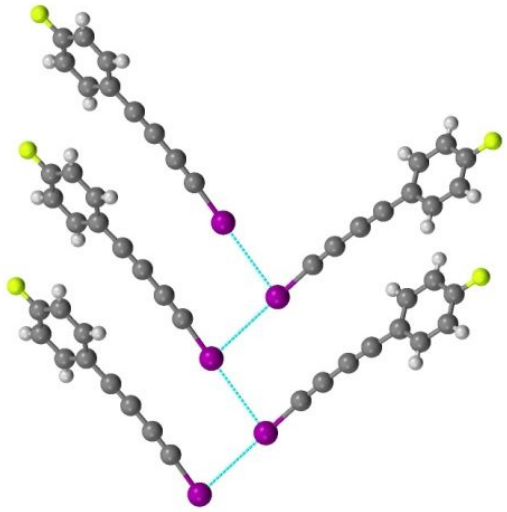

Figure 4. Crystal structure of **FC_4I**.

Different situation is observed in **$C_6F_5C_6I$** crystal structure (Figure 5), where there are no I···I contacts. Instead, strong π···π intractions between perfluorinated phenyl rings and polyyne chains are observed. Such contacts might be regarded as analogues of C_6H_6/C_6F_6 strong interactions[63-64] which are useful tool in crystal engineering.[65] CHELPG electrostatic potential calculations are in accordance with that (see Theoretical Calculations) and polyyne chain is electron deficient whereas there is a positive electrostatic potential on perfluorinated phenyl ring.

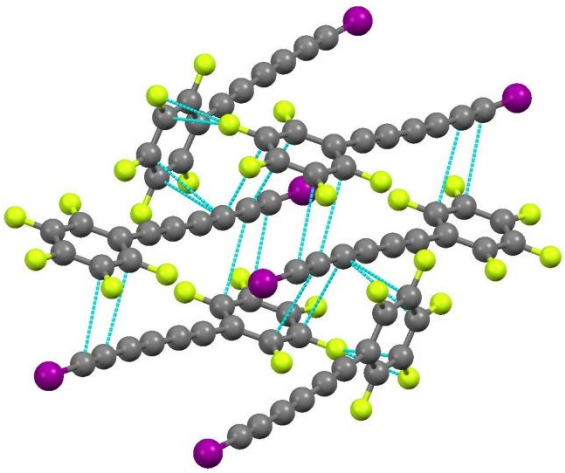

Figure 5. Crystal structure of **$C_6F_5C_6I$**.

Halogen bond plays a crucial role in intermolecular interactions in most of the structures. It is known that the polarizing effect of sp-carbon in combination with electron-withdrawing effect of phenyl ring substituent should lead to highly electrophilic halogen atoms and thus strong halogen bonds.[66-68] The geometrical parameters of the C≡CX···D interactions are summarized in the Table 3. The Cl···O halogen bond in the structure of 1-chlorobutadiyne (R_{XD} = 0.94) is significantly weaker than Br···O interaction in the 1-bromopolyynes (R_{XD} = 0.83-0.86). Since iodine forms stronger halogen bonds than bromine or chlorine it is not surprising that I···O and I···N interactions in the structures of 1-iodopolyynes are even stronger. Comparing to the literature such halogen bonds should be regarded as very strong.[69] Inspired by the fact that the length of C-I bond is influenced by the length of polyyne chain we decided to investigate an impact of chain length on I···N distance for **CNC_nI** series. The packing motif of **CNC_2I** crystal structure is similar to its longer homologues thus it was included in this analysis. The difference between I···N distance in **CNC_2I** (2.962(3) Å) and in the crystal structures for longer **CNC_nI** homologs (n = 4, 2.883(3) Å; n = 6, 2.881(2) Å; n = 8, 2.888(5) Å) is significant but this trend seems to be quickly saturated. Moreover, the shortening of Br···O interaction is observed for **NO_2C_4Br** and **NO_2C_6Br** pair (2.915 Å and 2.880 Å, respectively). The trend in Br···O interactions for **$MeC(O)C_4Br$** and **$MeC(O)C_6Br$** crystal structures is not so clear. The Br···O distance for **$MeC(O)C_4Br$** is 2.880(3) Å whereas in the crystal structure of **$MeC(O)C_6Br$** - where there are two molecules in two asymmetric unit - it is 2.815(2) Å or 2.894(2) Å.

Table 3. Geometrical parameters of halogen bonds in structures of 1-halopolyynes.

Compound	**X···D**	**sym. Equivalence**	**X···D [Å]**	**∠(CXD) [deg]**	**R_{XD} [%]**
$MeC(O)C_4Cl$	Cl···O	1+x,y,1+z	3.062(3)	173.07(13)	0.94
NO_2C_4Br	Br···O	-1+x,y,1+z	2.915(2)	174.10(5)	0.86

MeC(O)C$_4$Br	Br···O	1+x,y,1+z	2.880(3)	175.44(11)	0.85
NO$_2$C$_6$Br	Br···O	1-x,-1/2+y,3/2-z	2.880(3)	173.31(12)	0.85
MeC(O)C$_6$Br[a]	Br···O	2-x,1-y,-z	2.815(2)	179.89(10)	0.83
MeC(O)C$_6$Br[a]	Br···O	-x,-1/2+y,1/2-z	2.894(2)	173.14(10)	0.86
CNC$_2$I[25a]	I···N	-1+x, y, 1+z	2.962(3)	175.17(2)	0.84
CNC$_4$I	I···N	1+x,y,-1+z	2.883(3)	176.96(11)	0.82
NO$_2$C$_4$I	I···O	1+x,y,-1+z	2.935(3)	176.90(10)	0.84
CNC$_6$I	I···N	2+x,y,-1+z	2.881(2)	178.11(7)	0.82
CNC$_8$I	I···N	2+x,-1+y,1+z	2.888(5)	178.45(18)	0.82

[a]Two molecules in the asymmetric unit; [b]$R_{XD} = (X\cdots D)/(r_X + r_D)$ where r_X and r_D are the van der Waals radii.[70]

Theoretical Calculations.

We decided to calculate CHELPG electrostatic potentials (Charges from Electrostatic Potentials using a Grid based method) in order to investigate the ability for halogen bond formation for all 1-halopolyynes. Especially an impact of carbon chain length on electrostatic potential on halogen atom was interesting. Higher electrostatic potential should lead to stronger halogen bond with the same electron pair donor. CHELPG potentials are summarized in the Table 4, whereas electron density isosurface plots are shown in Figure 6. The experimental trend in the length of I···N interaction for **CNC$_n$I** series seems to be consistent with calculated CHELPG values. CHELPG value on iodine atom for **CNC$_2$I** is 0.163 whereas for longer analogues it is significantly higher (0.207, 0.210, 0.213 for n = 4, 6 and 8, respectively). This quick saturation of the trend is consistent with halogen bond lengths for this series of 1-halopolyynes (Table 4). An increase of electrostatic potential on halogen atoms with increasing carbon chain length is also observed for **MeC(O)C$_4$Br** and **MeC(O)C$_4$Br** pair (CHELPG = 0.159 and 0.175) as well as for **NO$_2$C$_4$Br** and **NO$_2$C$_6$Br** pair (CHELPG = 0.172 and 0.185). The NBO (Natural Bond Orbital) values are consistent with CHELPG values and the same trends are observed.

Table 4. The NBO (Natural Bond Orbital) charges and charges from electrostatic potentials (CHELPG) of halogen atoms.

Compound	NBO [e]	CHELPG [e]
$MeC(O)C_4Cl$	0.139	0.109
$MeC(O)C_4Br$	0.225	0.159
$MeC(O)C_6Br$	0.232	0.175
CNC_2I	0.344	0.163
CNC_4I	0.360	0.207
CNC_6I	0.367	0.210
CNC_8I	0.371	0.213
NO_2C_4I	0.129	0.361
NO_2C_4Br	0.231	0.172
NO_2C_6Br	0.237	0.185
FC_4I	0.349	0.179
$C_6F_5C_6I$	0.369	0.221

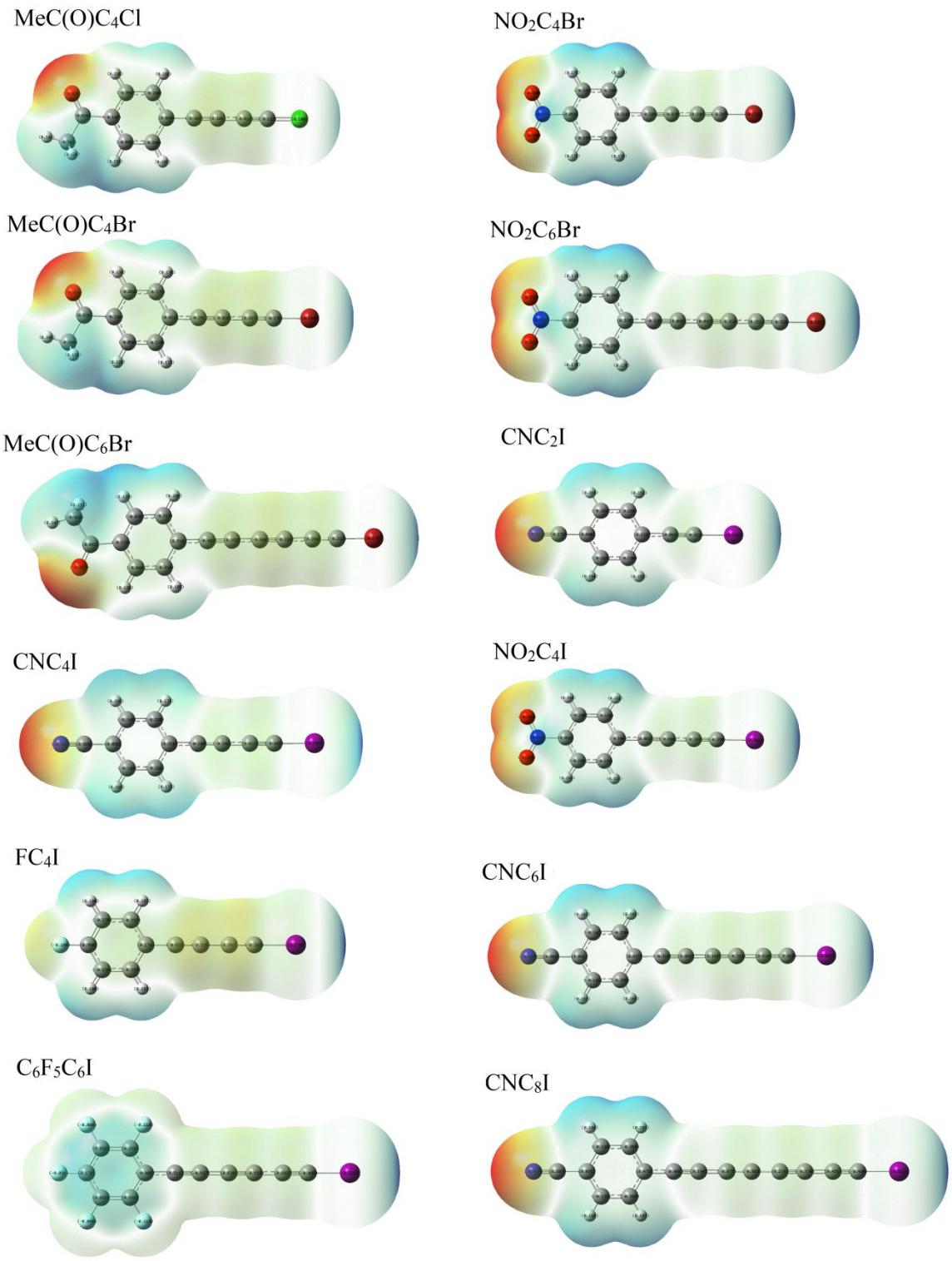

Figure 6. The charges from electrostatic potentials (CHELP) of 1-halopolyynes. The red color on electron density isosurface indicates maximum of negative values of electrostatic potential and the blue color indicates the maximum of positive electrostatic potential.

Hirshfeld Surface Analysis

The intermolecular contacts in the crystal structures of all 1-halopolyynes were analyzed by Hirshfeld surface studies using CrystalExplorer software.[71] The shape and size of Hirshfeld surface is related to the intermolecular contacts between atoms and in addition to that some properties (like curvature) may be encoded with the use of colors.[72] This analysis may be also visualized as two-dimensional (d_i, d_e) fingerprint graph.[73] Such graph brings more information than simple measurements of distances between atoms and is a perfect way to visualize various intermolecular interactions. Here d_{norm} values are encoded with colors: red – the highest value, blue – the lowest value.

The packing motifs of all 1-halopolyynes that have strong electron pair donor end-group (**MeC(O)C$_4$Cl**, **NO$_2$C$_4$Br**, **MeC(O)C$_4$Br**, **NO$_2$C$_6$Br**, **MeC(O)C$_6$Br**, **CNC$_4$I**, **NO$_2$C$_4$I**, **CNC$_6$I** and **CNC$_8$I**) are quite similar and their interactions are visible due to Hirshfeld surface analysis as well as related fingerprint plots are rather analogous. As an example, more detailed analysis was conducted here for **CNC$_8$I**. Hirshfeld surface plots and fingerprint graphs of all 1-halopolyynes are in the Supporting Information (Figures S13-S24). Fingerprints and Hirshfeld surface for **CNC$_8$I** are shown in Figure 7 (top). Main features of the fingerprint may be assigned to strong interactions. Strong C-I···N halogen bond is clearly visible on fingerprint plot as sharp spikes denoted with letter **a**. Moreover, weaker C_{sp2}-H···π(polyyne) interactions are visible as more blurred shapes that are denoted with letter **b**. Flat shape of molecule facilitates π···π interactions between polyyne systems that might be also visible on fingerprint plot (Figure 7, down).

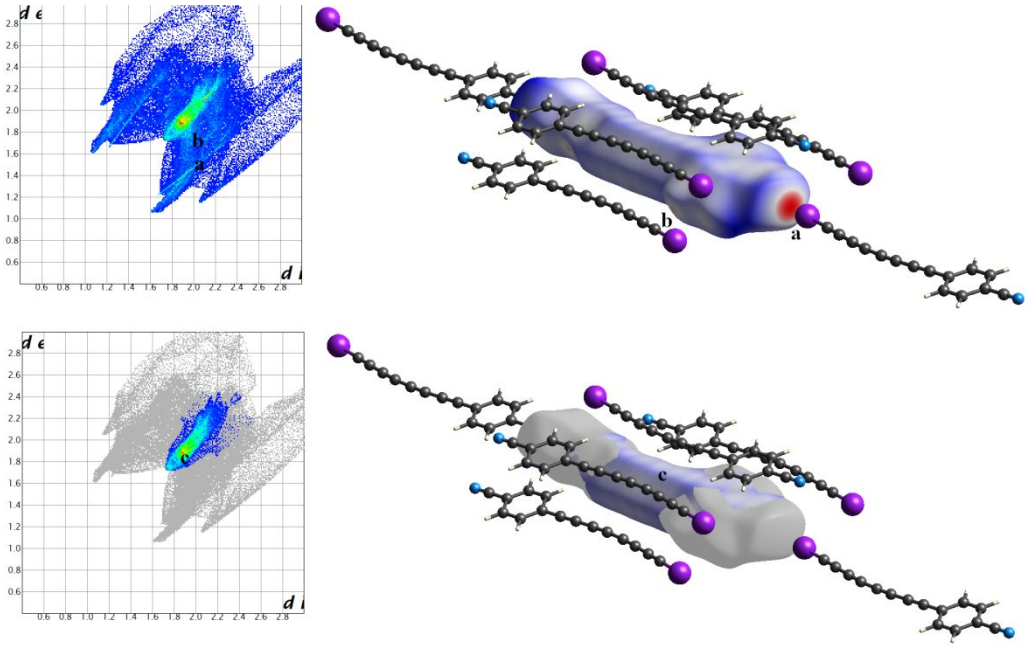

Figure 7. a) Fingerprint plot (upper, left) and Hirshfeld surface of **CNC$_8$I** (upper, right); b) fingerprint plot (lower, left)) and Hirshfeld surface of **CNC$_8$I** (lower, right) with π··π interaction underlined (down).

Intermolecular interactions in the structure of **FC$_4$I** are different than in structures with the presence of X···O or X···N halogen bonds. Significant I···I interactions **a** are visible as sharp needles on fingerprint plot (Figure 8). Also some alkyne π···H-C interactions might be observed as more blurred shapes **b**. Moreover, numerous weaker π···π stacking interactions are present in the crystal structure and are denoted with the letter **c**.

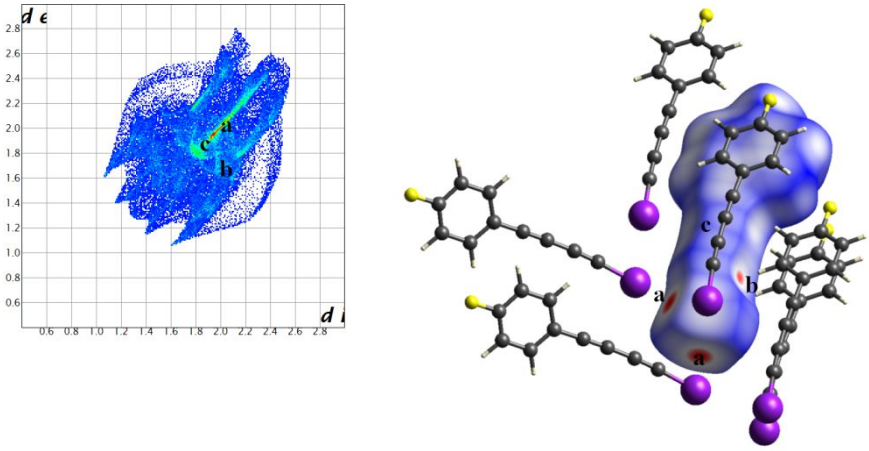

Figure 8. Fingerprint plot and Hirshfeld surface of **FC$_4$I**.

The situation is different when there is no possibility of halogen bond formation and other interactions start to play more important role. Fingerprint plot and Hirshfeld surface of $C_6F_5C_6I$ are shown in Figure 9. The C-F···I interactions are clearly visible as sharp spike on fingerprint plot and are denoted with the letter **a**. In addition to that few F···F interactions may be observed (**b**). In this case the flat shape of the molecule as well as high affinity of C_6F_5 moiety to electron poor polyyne chains also facilitates close and strong π···π contacts denoted here with letter **c**. The strongest π···π interactions are observed between C_6F_5 moiety and the electron poor polyyne chain of the other molecule. Moreover, some C-F···π contacts may be observed (**d**).

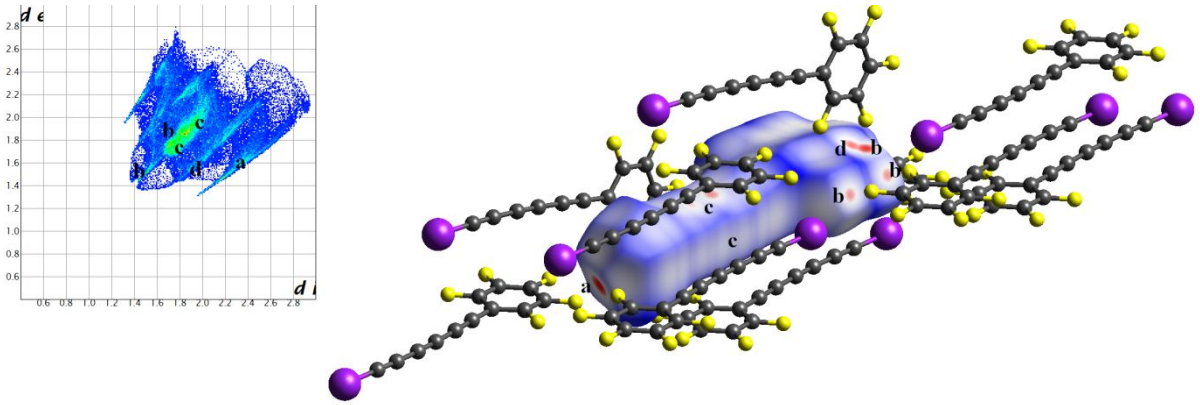

Figure 9. Fingerprint plot and Hirshfeld surface of **$C_6F_5C_6I$**.

CONCLUSIONS

We have reported 11 new crystal structures of 1-halopolyynes greatly increasing the number of such compounds characterized by X-ray single crystal diffraction. Compound **CNC_8I** is the longest known 1-halopolyyne characterized with the use of such method to date. Moreover, the first two crystal structures of 1-bromohexatriynes were reported herein. The impact of an end-group on packing was analyzed and if halogen bond acceptor end-group is used then crystal structure might be predicted with good accuracy. In other cases halogen-halogen or π-π interactions may start to play more crucial role. An influence of the length of

sp-hybridized carbon chain on the C-X bond distance was analyzed. Longer polyyne chain means stronger halogen bond formed by 1-halopolyyne. However, this trend seems to be quite quickly saturated and the biggest difference is between simple 1-haloalkyne and 1-halobutadiyne. This might be important information in future prediction of crystal structures for new 1-halopolyynes.

ASSOCIATED CONTENT

The Supporting Information is available free of charge on the ACS Publications website at DOI: .

X-ray crystallography details, molecular structures of 1-halopolyynes, Hirshfeld surfaces, calculated bond lengths, and NMR spectra of all new compounds (PDF)

Accession Codes CCDC 1866791-1866801 contain the supplementary crystallographic data for this paper. These data can be obtained free of charge via www.ccdc.cam.ac.uk/data_request/cif, or by emailing data_request@ccdc.cam.ac.uk, or by contacting The Cambridge Crystallographic Data Centre, 12 Union Road, Cambridge CB2 1EZ, UK; fax: +44 1223 336033.

AUTHOR INFORMATION

Corresponding Authors

*(S.S.) E-mail: slawomir.szafert@chem.uni.wroc.pl

*(B.P.) E-mail: bartlomiej.pigulski@chem.uni.wroc.pl

ORCID

Bartłomiej Pigulski: 0000-0002-9925-2878

Sławomir Szafert: 0000-0002-0570-884

Author Contributions

The manuscript was written through contributions of all authors. All authors have given approval to the final version of the manuscript.

ACKNOWLEDGMENT

The authors would like to thank the National Science Centre Poland (Grants UMO-2015/19/B/ST5/02917 and UMO-2017/25/N/ST5/01062) and the National Centre for Research and Development (Grant TANGO1/266660/NCBR/2015) for support of this research.

REFERENCES

1. Haley, M. M.; Tykwinski, R. R., *Carbon Rich Compounds: From Molecules to Materials*. Wiley-VCH: Weinheim, 2005.

2. Diederich, F.; Stang, P. J.; Tykwinski, R. R., *Acetylene Chemistry: Chemistry, Biology and Material Science*. Wiley-VCH: Weinheim, 2005.

3. Cataldo, F. E., *Polyynes: Synthesis Properties and Applications*. CRC Press Taylor & Francis Group: Boca Raton, 2006.

4. Chalifoux, W. A.; Tykwinski, R. R., Synthesis of polyynes to model the sp-carbon allotrope carbyne. *Nat. Chem.* **2010**, *2*, 967-971.

5. Szafert, S.; Gladysz, J. A., Carbon in One Dimension: Structural Analysis of the Higher Conjugated Polyynes. *Chem. Rev.* **2003**, *103*, 4175-4206.

6. Szafert, S.; Gladysz, J. A., Update 1 of: Carbon in One Dimension: Structural Analysis of the Higher Conjugated Polyynes. *Chem. Rev.* **2006**, *106*, PR1-PR33.

7. Chalifoux, W. A.; McDonald, R.; Ferguson, M. J.; Tykwinski, R. R., *tert*-Butyl-End-Capped Polyynes: Crystallographic Evidence of Reduced Bond-Length Alternation. *Angew. Chem. Int. Ed.* **2009**, *48*, 7915-7919.

8. Pigulski, B.; Gulia, N.; Szafert, S., Reactivity of Polyynes: Complex Molecules from Simple Carbon Rods. *Eur. J. Org. Chem.* **2019**, 1420-1445.

9. Moreno-García, P.; Gulcur, M.; Manrique, D. Z.; Pope, T.; Hong, W.; Kaliginedi, V.; Huang, C.; Batsanov, A. S.; Bryce, M. R.; Lambert, C.; Wandlowski, T., Single-Molecule Conductance of Functionalized Oligoynes: Length Dependence and Junction Evolution. *J. Am. Chem. Soc.* **2013**, *135*, 12228-12240.

10. Gulcur, M.; Moreno-García, P.; Zhao, X.; Baghernejad, M.; Batsanov, A. S.; Hong, W.; Bryce, M. R.; Wandlowski, T., The Synthesis of Functionalised Diaryltetraynes and Their Transport Properties in Single-Molecule Junctions. *Chem. Eur. J.* **2014**, *20*, 4653-4660.

11. Schwarz, F.; Kastlunger, G.; Lissel, F.; Riel, H.; Venkatesan, K.; Berke, H.; Stadler, R.; Lörtcher, E., High-Conductive Organometallic Molecular Wires with Delocalized Electron Systems Strongly Coupled to Metal Electrodes. *Nano Lett.* **2014**, *14*, 5932-5940.

12. Lissel, F.; Schwarz, F.; Blacque, O.; Riel, H.; Lörtscher, E.; Venkatesan, K.; Berke, H., Organometallic Single-Molecule Electronics: Tuning Electron Transport through X(diphosphine)$_2$FeC$_4$Fe(diphosphine)$_2$X Building Blocks by Varying the Fe–X–Au Anchoring Scheme from Coordinative to Covalent. *J. Am. Chem. Soc.* **2014**, *136*, 14560-14569.

13. Milan, D. C.; Krempe, M.; Ismael, A. K.; Movsisyan, L. D.; Franz, M.; Grace, I.; Brooke, R. J.; Schwarzer, W.; Higgins, S. J.; Anderson, H. L.; Lambert, C. J.; Tykwinski, R.

R.; Nichols, R. J., The single-molecule electrical conductance of a rotaxane-hexayne supramolecular assembly. *Nanoscale* **2017**, *9*, 355-361.

14. Slepkov, A. D.; Hegmann, F. A.; Eisler, S.; Elliot, E.; Tykwinski, R. R., The surprising nonlinear optical properties of conjugated polyyne oligomers. *J. Phys. Chem.* **2004**, *120*, 6807-6810.

15. Eisler, S.; Slepkov, A. D.; Elliott, E.; Luu, T.; McDonald, R.; Hegmann, F. A.; Tykwinski, R. R., Polyynes as a Model for Carbyne: Synthesis, Physical Properties, and Nonlinear Optical Response. *J. Am. Chem. Soc.* **2005**, *127*, 2666-2676.

16. Xu, G.-L.; Wang, C.-Y.; Ni, Y.-H.; Goodson III, T. G.; Ren, T., Iterative Synthesis of Oligoynes Capped by a $Ru_2(ap)_4$-terminus and Their Electrochemical and Optoelectronic Properties. *Organometallics* **2005**, *24*, 3247-3254.

17. Samoc, M.; Dalton, G. T.; Gladysz, J. A.; Zheng, Q.; Velkov, Y.; Agren, H.; Norman, P.; Humphrey, M. G., Cubic Nonlinear Optical Properties of Platinum-Terminated Polyynediyl Chains. *Inorg. Chem.* **2008**, *47*, 9946-9957.

18. Stefko, M.; Tzirakis, M. D.; Breiten, B.; Ebert, M.-O.; Dumele, O.; Schweizer, W. B.; Gisselbrecht, J. P.; Boudon, C.; Beels, M. T.; Biaggio, I.; Diederich, F., Donor-Acceptor (D-A)-Substituted Polyyne Chromophores: Modulation of Their Optoelectronic Properties by Varying the Length of the Acetylene Spacer. *Chem. Eur. J.* **2013**, *19*, 12693-12704.

19. Arendt, A.; Kołkowski, R.; Samoc, M.; Szafert, S., Spectral dependence of nonlinear optical properties of symmetrical octatetraynes with p-substituted phenyl end-groups. *Phys. Chem. Chem. Phys.* **2015**, *17*, 13680-13688.

20. Agarwal, N. R.; Lucotti, A.; Tommasini, M.; Chalifoux, W. A.; Tykwinski, R. R., Nonlinear Optical Properties of Polyynes: An Experimental Prediction for Carbyne. *J. Phys. Chem. C* **2016**, *120*, 11131-11139.

21. Hu, F.; Zeng, C.; Long, R.; Miao, Y.; Wei, L.; Xu, Q.; Min, W., Supermultiplexed optical imaging and barcoding with engineered polyynes. *Nat. Methods* **2018**, *15*, 194-200.

22. Shi Shun, A. L. K.; Tykwinski, R. R., Synthesis of Naturally Occurring Polyynes. *Angew. Chem. Int. Ed.* **2006**, *45*, 1034-1057.

23. Liu, M.; Artyukhov, V. I.; Lee, H.; Xu, F.; Yakobson, B. I., Carbyne from First Principles: Chain of C Atoms, a Nanorod or a Nanorope. *Acs Nano* **2013**, *7*, 10075-10082.

24. Shi, L.; Rohringer, P.; Suenaga, K.; Niimi, Y.; Kotakoski, J.; Meyer, J. C.; Peterlik, H.; Wanko, M.; Cahangirov, S.; Rubio, A.; Lapin, Z. J.; Novotny, L.; Ayala, P.; Pichler, T., Confined linear carbon chains as a route to bulk carbyne. *Nature Materials* **2016**, *15*, 634-639.

25. Pavliček, N.; Gawel, P.; Kohn, D. R.; Majzik, Z.; Xiong, Y.; Meyer, G.; Anderson, H. L.; Gross, L., Polyyne formation via skeletal rearrangement induced by atomic manipulation. *Nat. Chem.* **2018**, *10*, 853-858.

26. Tomilin, D. N.; Pigulski, B.; Gulia, N.; Arendt, A.; Sobenina, L. N.; Mikhaleva, A. I.; Szafert, S.; Trofimov, B. A., Direct synthesis of butadiynyl-substituted pyrroles under solvent- and transition metal-free conditions. *RSC Adv.* **2015**, *5*, 73241-73248.

27. Pigulski, B.; Arendt, A.; Tomilin, D. N.; Sobenina, L. N.; Trofimov, B. A.; Szafert, S., Transition-Metal Free Mechanochemical Approach to Polyyne Substituted Pyrroles. *J. Org. Chem.* **2016,** *81*, 9188-9198.

28. Pigulski, B.; Męcik, P.; Cichos, J.; Szafert, S., Use of Stable Amine-Capped Polyynes in the Regioselective Synthesis of Push–Pull Thiophenes. *J. Org. Chem.* **2017**, *82*, 1487-1498.

29. Feustel, M.; Himbert, G., Nicht-symmetrische (butadiin)diamine. *Tetrahedron Lett.* **1965**, *24*, 2165-2168.

30. Kerisit, N.; Toupet, L.; Larini, P.; Perrin, L.; Guillemin, J.-C.; Trolez, Y., Straightforward Synthesis of 5-Bromopenta-2,4-diynenitrile and Its Reactivity Towards Terminal Alkynes: A Direct Access to Diene and Benzofulvene Scaffolds. *Chem. Eur. J.* **2015**, *21*, 6042-6047.

31. Kerisit, N.; Ligny, Romain; Gauthier, E. S.; Guegan, J.-P.; Toupet, L.; Guillemin, J.-C.; Trolez, Y., Synthesis and Reactivity of 5-Bromopenta-2,4-diynenitrile (BrC5N): an Access to π-Conjugated Scaffolds. *Helv. Chim. Acta* **2019**, *102*, e1800232.

32. Pigulski, B.; Cichos, J.; Szafert, S., Polyynes as Precursors of Photoluminescent Solvent Polarity Probes. *ACS Sustain. Chem. Eng.* **2017**, *5*, 7077-7085.

33. Gulia, N.; Pigulski, B.; Szafert, S., Palladium End-Capped Polyynes via Oxidative Addition of 1-Haloalkynes to $Pd(PPh_3)_4$, *Organometallics* **2015**, *34*, 673-682.

34. Pigulski, B.; Gulia, N.; Szafert, S., Synthesis of Long, Palladium End-Capped Polyynes through the Use of Asymmetric 1-Iodopolyynes. *Chem. Eur. J.* **2015**, *21*, 17769-17778.

35. Pigulski, B.; Jarszak, A.; Szafert, S., Selective synthesis of iridium(III) end-capped polyynes by oxidative addition of 1-iodopolyynes to Vaska's complex. *Dalton Trans.* **2018**, *47*, 17046-17054.

36. Groom, C. R.; Bruno, I. J.; Lightfoot, M. P.; Ward, S. C., The Cambridge Structural Database. *Acta Crysta.* **2016**, *B72*, 171-179.

37. Baillargeon, P.; Rahem, T.; Caron-Duval, É.; Tremblay, J.; Fortin, C.; Blais, É.; Fan, V.; Fortin, D.; Y. L. Dory, Isomorphous crystal structures of chlorodiacetylene and iododiacetylene derivatives: simultaneous hydrogen and halogen bonds on carbonyl. *Acta Cryst.* **2017**, *E73*, 1175-1179.

38. Hoheisel, N.; Schrettl, S.; Marty, R.; Todorova, T. K.; Corminboeuf, C.; Sienkiewicz, A.; Scopelliti, R.; Schweizer, W. B.; Frauenrath, H., A multistep single-crystal-to-single-crystal bromodiacetylene dimerization. *Nat. Chem.* **2013**, *5*, 327-334.

39. Jin, H.; Young, C. N.; Halada, G. P.; Philips, B. L.; Goroff, N. S., Synthesis of the Stable Ordered Conjugated Polymer Poly(dibromodiacetylene) from an Explosive Monomer. *Angew. Chem. Int. Ed.* **2015**, *54*, 14690-14695.

40. Baillargeon, P.; Caron-Duval, É.; Pellerin, É.; Gagné, S.; Dory, Y. L., Isomorphous Crystals from Diynes and Bromodiynes Involved in Hydrogen and Halogen Bonds. *Crystals* **2016**, *6*, 37.

41. Dikarev, E. V.; Goroff, N. S.; Petrukhina, M. A., Expanding the scope of solvent-free synthesis: entrapment of thermally unstable species. *J. Organomet. Chem.* **2003**, *683*, 337-340.

42. Goroff, N. S.; Curtis, S. M.; Webb, J. A.; Fowler, F. W.; Lauher, J. W., Designed Cocrystals Based on the Pyridine−Iodoalkyne Halogen Bond. *Org. Lett.* **2005**, *7*, 1891-1893.

43. Sun, A.; Lauher, J. W.; Goroff, N. S., Preparation of Poly(diiododiacetylene), an Ordered Conjugated Polymer of Carbon and Iodine. *Science* **2006**, *312*, 1030-1034.

44. Luo, L.; Wilhelm, C.; Sun, A.; Grey, C. P.; Lauher, J. W.; Goroff, N. S., Poly(diiododiacetylene): Preparation, Isolation, and Full Characterization of a Very Simple Poly(diacetylene). *J. Am. Chem. Soc.* **2008**, *130*, 7702-7709.

45. Wilhelm, C.; Boyd, S. A.; Chawda, S.; Fowler, F. W.; Goroff, N. S.; Halada, G. P.; Grey, C. P.; Lauher, J. W.; Luo, L.; Martin, C. D.; Parise, J. B.; Tarabrella, C.; Webb, J. A., Pressure-Induced Polymerization of Diiodobutadiyne in Assembled Cocrystals. *J. Am. Chem. Soc.* **2008**, *130*, 4415-4420.

46. Eichstaed, K.; Wicher, B.; Gdaniec, M.; Połoński, T., Halogen bonded polypseudorotaxanes based on a pillar[5]arene host. *CrystEngComm* **2016**, *18*, 5807-5810.

47. Gao, K.; Goroff, N. S., Two new iodine-capped carbon rods. *J. Am. Chem. Soc.* **2000**, *122*, 9320-9321.

48. Cavallo, C.; Metrangolo, P.; Milani, R.; Pilati, T.; Priimagi, A.; Resnati, G.; Terraneo, G., The Halogen Bond. *Chem. Rev.* **2016**, *116*, 2478-2601.

49. Lauher, J. W.; Fowler, F. W.; Goroff, N. S., Single-Crystal-to-Single-Crystal Topochemical Polymerizations by Design. *Acc. Chem. Res.* **2008**, *41*, 1215-1229.

50. Gulia, N.; Pigulski, B.; Charewicz, M.; Szafert, S., A Versatile and Highly Efficient Method for 1-Chlorination of Terminal and Trialkylsilyl-Protected Alkynes. *Chem. Eur. J.* **2014**, *20*, 2746-2749.

51. Dumele, O.; Wu, D.; Trapp, N.; Goroff, N.; Diederich, F., Halogen Bonding of (Iodoethynyl)benzene Derivatives in Solution. *Org. Lett.* **2014**, *16*, 4722-4725.

52. Chen, X.; Merrett, J. T.; Chan, P. W. H., Gold-Catalyzed Formal [4 + 2] Cycloaddition of 5-(Ethynylamino)pent-2-yn-1-yl Esters to 1,2,3,5-Tetrahydrobenzo[*g*]quinolines. *Org. Lett.* **2018**, *20*, 1542-1545.

53. Sheldrick, G. M., A short history of SHELX. *Acta Crystallogr. A* **2008**, *64*, 112-122.

54. Agilent (2014). *CrysAlis PRO*. Agilent Technologies Ltd, Yarnton, Oxfordshire, England.

55. Macrae, C. F.; Edgington, P. R.; McCabe, P.; Pidcock, E.; Shields, G. P.; Taylor, R.; Towler, M.; van de Streek, J., Mercury: visualization and analysis of crystal structures *J. Appl. Cryst.* **2006**, *39*, 453-457.

56. Frisch, M. J.; Trucks, G. W.; Schlegel, H. B.; Scuseria, G. E.; Robb, M. A.; Cheeseman, J. R.; Scalmani, G.; Barone, V.; Mennucci, B.; Petersson, G. A.; Nakatsuji, H.; Caricato, M.; Li, X.; Hratchian, H. P.; Izmaylov, A. F.; Bloino, J.; Zheng, G.; Sonnenberg, J. L.; Hada, M.; Ehara, M.; Toyota, K.; Fukuda, R.; Hasegawa, J.; Ishida, M.; Nakajima, T.; Honda, Y.; Kitao, O.; Nakai, H.; Vreven, T.; J. A. Montgomery, J.; Peralta, J. E.; Ogliaro, F.; Bearpark, M.; Heyd, J. J.; Brothers, E.; Kudin, K. N.; Staroverov, V. N.; Kobayashi, R.; Normand, J.; Rendell, K. R. A.; Burant, J. C.; Iyengar, S. S.; Tomasi, J.; Cossi, M.; Rega, N.; Millam, J. M.; Klene, M.; Knox, J. E.; Cross, J. B.; Bakken, V.; Adamo, C.; Jaramillo, J.; Gomperts, R.; Stratmann, R. E.; Yazyev, O.; Austin, A. J.; Cammi, R.; Pomelli, C.; Ochterski, J. W.; Martin, R. L.; Morokuma, K.; Zakrzewski, V. G.; Voth, G. A.; Salvador, P.; Dannenberg, J. J.; Dapprich, S.; Daniels, A. D.; Farkas, Ö.; Foresman, J. B.; Ortiz, J. V.; Cioslowski, J.; Fox, D. J. *Gaussian 09, Revision*, Gaussian Inc.: Wallingford CT, 2009.

57. Chai, J.-D.; Head-Gordon, M., Long-range corrected hybrid density functionals with damped atom-atom dispersion corretions. *Phys. Chem. Chem. Phys.* **2008**, *10*, 6615-6620.

58. Singh, U. C.; Kollman, P. A., An approach to computing electrostatic charges for molecules. *J. Comp. Chem.* **1984**, *5*, 129-145.

59. Besler, B. H.; K. M. Merz, J.; Kollman, P. A., Atomic charges derived from semiempirical methods. *J. Comp. Chem.* **1990**, *11*, 431-439.

60. Rappe, A. K.; Casewit, C. J.; Colwell, K. S.; Goddard III, W. A.; Skiff, W. M., UFF, a full periodic table force field for molecular mechanics and molecular dynamics simulations. *J. Am. Chem. Soc.* **1990**, *114*, 10024-10035.

61. Dennington, R.; Keith, T. A.; Millam, J. M. *GaussView, version 5*, Semichem Inc.: Shawnee Mission, KS, 2008.

62. Wolff, S. K.; Grimwood, D. J.; McKinnon, J. J.; Turner, M. J.; Jayatiala, D.; Spackman, M. A. *CrystalExplorer (Version 3.1)*, University of Western Austalia: 2012.

63. Williams, J. H., The molecular electric quadrupole moment and solid-state architecture. *Acc. Chem. Res.* **1993**, *26*, 593-598.

64. Patrick, C. R.; Prosser, G. S., A Molecular Complex of Benzene and Hexafluorobenzene. *Nature* **1960**, *187*, 1021.

65. Kendall, J.; McDonald, R.; Ferguson, M. J.; Tykwinski, R. R., Synthesis and Solid-State Structure of Perfluorophenyl End-Capped Polyynes. *Org. Lett.* **2008**, *10*, 2163-2166.

66. Aakeröy, C. B.; Wijethunga, T. K.; Desper, J.; Daković, M., Crystal Engineering with Iodoethynylnitrobenzenes: A Group of Highly Effective Halogen-Bond Donors. *Cryst. Growth Des.* **2015**, *15*, 3853-3861.

67. Aakeröy, C. B.; Baldrighi, M.; Desper, J.; Metrangolo, P.; Resnati, G., Supramolecular Hierarchy among Halogen-Bond Donors. *Chem. Eur. J.* **2013**, *19*, 16240-16247.

68. Metrangolo, P.; Meyer, F.; Pilati, T.; Resnati, G.; Terraneo, G., Halogen Bonding in Supramolecular Chemistry. *Angew. Chem. Int. Ed.* **2008**, *47*, 6114-6127.

69. Metrangolo, P.; Neukirch, H.; Pilati, T.; Resnati, G., Halogen Bonding Based Recognition Processes: A World Parallel to Hydrogen Bonding. *Acc. Chem. Res.* **2005**, *38*, 386-395.

70. Bondi, A., Van der Waals Volumes ans Radii. *J. Phys. Chem.* **1964**, *68*, 441-451.

71. McKinnon, J. J.; Jayatilaka, D.; Spackman, M. A., Towards quantitative analysis of intermolecular interactions with Hirshfeld surfaces. *Chem. Commun.* **2007**, 3814-3816.

72. Spackman, M. A.; Jayatilaka, D., Hirshfeld surface analysis. *CrystEngComm.* **2009**, *11*, 19-32.

73. Spackman, M. A.; McKinnon, J. J., Fingerprinting intermolecular interactions in molecular crystals. *CrystEngComm.* **2002**, *4*, 378-392.

For Table of Contents Use Only

Crystal Engineering of 1-Halopolyynes by End-Group Manipulation

Bartłomiej Pigulski, Nurbey Gulia, Patrycja Męcik, Robert Wieczorek, Agata Arendt, Sławomir Szafert**

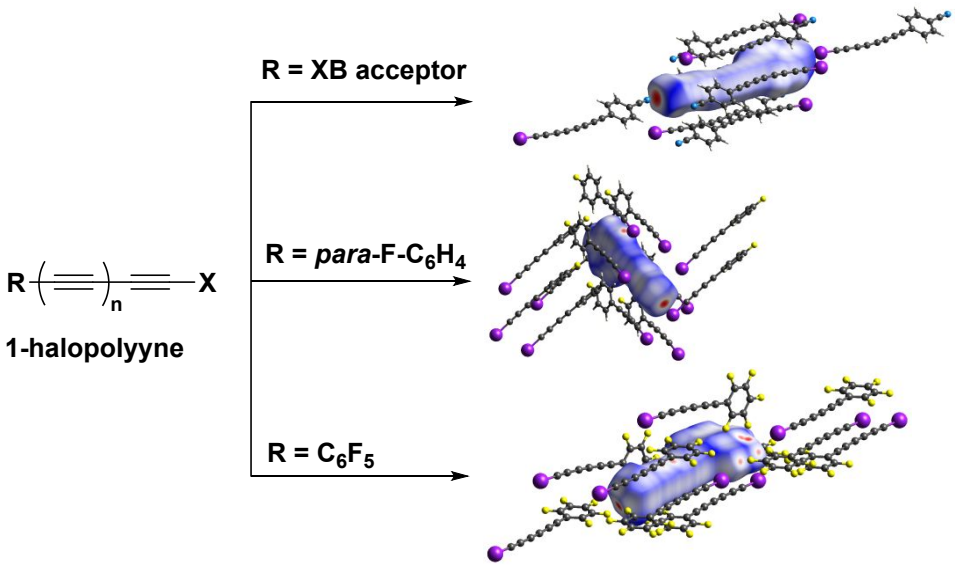

Synopsis: A series of 11 X-ray crystal structures of 1-halpolyynes has been reported including the first structures containing $(C{\equiv}C)_4I$ and $(C{\equiv}C)_3Br$ structural motifs. The influence of the end-group type on packing was thoroughly analyzed with the support of theoretical calculations.